

**Modeling the Effect of Hydrogeochemical Evolution on Concrete Degradation in the Proposed LLW Disposal Site of Taiwan - 11253**

Wen-Sheng Lin<sup>1</sup>, Chen-Wuing Liu<sup>2</sup>, Ming-Hsu Li<sup>3</sup>

<sup>1</sup>Hydrotech Research Institute, National Taiwan University, Taipei, Taiwan

<sup>2</sup>Department of Bioenvironmental Systems Engineering, National Taiwan University, Taipei, Taiwan

<sup>3</sup>Institute of Hydrological and Oceanic Sciences, National Central University, Jhongli, Taiwan

**ABSTRACT**

Many disposal concepts currently show that concrete is an effective confinement material used in engineered barrier system (EBS) at a number of LLW disposal sites. Cement-based materials have properties for the encapsulation, isolation, or retardation of a variety of hazardous contaminants. However, several questions are raised about the safety of concrete barrier, such as: Could the EBS completely isolate from groundwater? What hydrogeochemical reactions and key aqueous species in ground water affect the degradation of concrete barrier of repository? How the redox processes influence on the formations of degradation materials? To evaluate the geochemical evolution of concrete barrier, reactive chemical transport, and groundwater flow models can be an effective tool. The present study aims to assess hydrogeochemical influences on concrete barrier degradation using reactive chemical transport model with thermodynamic equilibria data in cementitious media. A proposed site for final disposal of LLW located in Daren Township of Taitung County along the southeastern coast has been on the selected list in Taiwan. Concrete is the confinement material in EBS of the proposed site. The reactive chemical transport model of HYDROGEOCHEM5.0 is applied to simulate the effect of hydrogeochemical processes on concrete barrier degradation in the proposed site. Simulated results show that the main processes responsible for concrete degradation are species induced from hydrogen ion, sulfate and chloride. The EBS with the side ditch drainage system can effectively discharge the infiltrated water and lower the solute concentrations that may induce the concrete degradation. Reductive environment in the EBS reduce the formation of ettringite formation in the concrete degradation processes. Moreover, the chemical conditions in the concrete barriers maintain alkaline condition after 300 years in proposed LLW repository site. This study provides a detailed picture of the long-term evolution of the hydrogeochemical environment in the proposed LLW disposal site in Taiwan.

**INTRODUCTION**

In Taiwan, low-level radioactive waste (LLW) is generated from a variety of commercial, medical, industrial, and educational activities. LLW is currently deposited inside nuclear power plants and at the storage site in Lanyu Island

temporarily. Site selection for LLW disposal is a challenge task. Concerns generally on the natural barriers are: What are the hydrogeological conditions favorable for the waste disposal? How frequent earthquakes, floods and humid environment affect the performance of engineering barrier system? Two disposal concepts including near-surface disposal design and mined cavern design with tunnel system are proposed. One potential site locates at a Dongjiyu islet of Penghu County. The site is composed of basaltic lavas with minor amounts of sedimentary rocks and uses a near-surface disposal design. However, the Dongjiyu islet is delineated as a Nature Reservation Area in 2009 and the siting process is aborted. The other proposed site located in Nanten Village, Daren Township of Taitung County. The geology of Daren site consists of argillite and meta-sedimentary rocks. A mined cavern design with a tunnel system of 500 m below the surface is proposed. Concrete is used as the confinement material for engineered barrier [1].

Concrete may be subject to degrade its strength by re-crystallisation and chemical interaction with the aqueous environment in the hydrogeochemical transport processes [2]. A number of reactions may take place simultaneously in groundwater and cement-based materials including hydrogen ion generated from dissolution of portlandite, increase of the concentration of calcium in the pore solution, formation of ettringite by sulfate attacking on concrete, and dissolution of chloride by pore water with the CSH gel and forming Friedel's salt [3]. Moreover, Bruno et al. [4] pointed out that the interaction of pore water with accessory minerals of bentonite controlled the geochemical characteristics of the system, such as sulfate dissolution-precipitation, and pyrite oxidation. Conversion of sulfide to sulfate concomitantly occurs with pyrite oxidation. Thus, redox processes may pronouncedly influence on the formations of degradation materials.

Cement-based materials can encapsulate, isolate, or retard a variety of hazardous contaminants. However, hydrogeochemical environment of LLW repository is governed by the composition of groundwater and mineral formation which may influence the chemical compatibility of backfill material, concrete barrier, and buffer material in the near field. Concrete is used as a confinement material in EBS at a number of LLW disposal sites. The durability of cementitious material in service environments is widely discussed, such as: Could the EBS completely isolate from groundwater? What hydrogeochemical reactions and key aqueous species in ground water affect the degradation of concrete barrier of repository? How the redox processes influence on the formations of degradation materials? Numerical model is an effective tool to evaluate the geochemical evolution of EBS, reactive transport of solute, and groundwater flow in the LLW disposal sites. The present study aims to assess the hydrogeochemical influences on concrete barrier degradation using reactive chemical transport model with thermodynamic equilibria data in cementitious media. The results of this study may answer various questions of long-term behavior of EBS in the proposed sites and provide a detailed picture of the long-term evolution of the hydrogeochemical environment of the proposed LLW disposal sites in Taiwan.

## **CONCRETE BARRIER**

Concrete majorly constitutes by a mixture of cement, water, and aggregates. The aggregates consist of minerals such as sand, gravel, and stone, which are chemically inert to water and concrete solid. The mineral compounds in cement

are calcium silicates ( $\text{Ca}_3\text{SiO}_5$  and  $\text{Ca}_2\text{SiO}_4$ ), aluminate ( $\text{Ca}_3\text{Al}_2\text{O}_6$ ), and ferrite ( $4\text{CaO} \cdot \text{Al}_2\text{O}_3 \cdot \text{Fe}_2\text{O}_3$ ) abbreviated as  $\text{C}_3\text{S}$ ,  $\text{C}_2\text{S}$ ,  $\text{C}_3\text{A}$  and  $\text{C}_4\text{AF}$ . As these constituents mix with water, calcium-silicate-hydrate (C-S-H), portlandite ( $\text{Ca}(\text{OH})_{2(s)}$ ), ettringite (Aft), monosulfate (AFm), hydrogarnet etc. will form in the cement hydration process. These hydration products are also control the setting and hardening of concrete. These alterations have direct consequences on the engineering properties of the concrete barrier. Figure 1 schematically illustrates the design of engineered barrier in the proposed Daren site. The thickness of concrete barrier ranges from 0.5 m to 1.0 m. The inner and outer thicknesses of bentonite buffer are 0.5 m and 0.2 m, respectively.

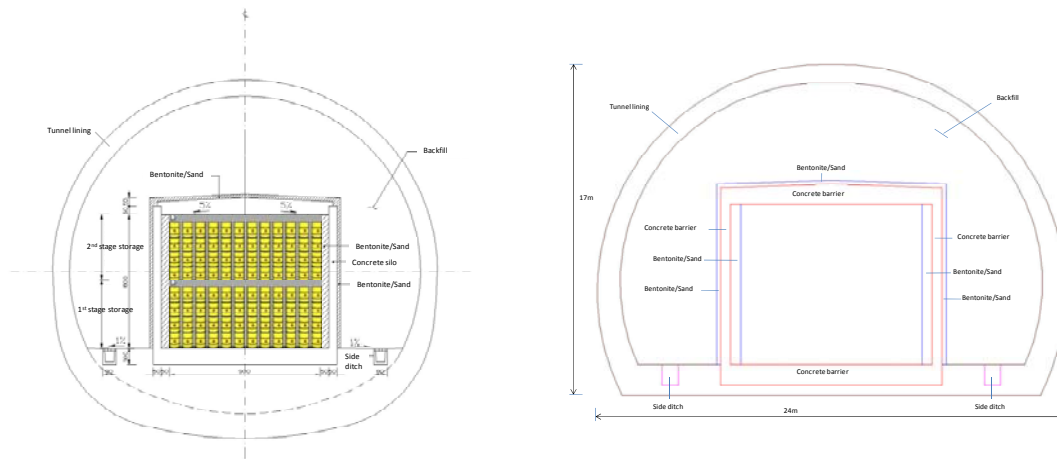


Fig. 1 Schematic illustration of the EBS design in the proposed site.

The chemical composition of Taiwan Cement and the calculated amount of the clinker phases in the unhydrated cement used in this study are listed in Table I. The mixed proportion of concrete components and their physical properties are summarized in Table II.

Table I Chemical Composition and Corresponding Clinker Phases in Taiwan Cement.

Component	Content % by Weight
CaO	61.96
SiO <sub>2</sub>	20.42
Al <sub>2</sub> O <sub>3</sub>	4.95
Fe <sub>2</sub> O <sub>3</sub>	3.09
MgO	3.29
Na <sub>2</sub> O+0.685 K <sub>2</sub> O	Max. 0.6
SO <sub>3</sub>	2.4
Corresponding clinker component	

Table II  
of Concrete  
their Physical

Tricalcium silicate ( $C_3S$ )	49
Dicalcium silicate ( $C_2S$ )	21
Tricalcium aluminate ( $C_3A$ )	7.9
Tetracalcium aluminate ferrite ( $C_4AF$ )	9.4
<b>Abbreviations used as following:</b> C=CaO, S=SiO <sub>2</sub> , A=Al <sub>2</sub> O <sub>3</sub> , F=Fe <sub>2</sub> O <sub>3</sub> , H=H <sub>2</sub> O	

Mixed Proportion  
Components and  
Properties.

Component	Content % by Volume
Cement +Water	30
Ballast	70
Physical Properties	Parameter
Density	2030kg/m <sup>3</sup>
w/c ratio	0.5
Porosity	0.15

## MODELING APPROACH

The composition and phase development of hydration products as cement's chemical reacting with groundwater flow influence the lifetime performance of the concrete barrier. Thermodynamic modeling of Portland cement in subsurface system of cementitious media were developed and applied to assess the performance of concrete barriers. Blanc et al. [5][6] has established thermodynamic data of chemical model for the phases of system CaO-SiO<sub>2</sub>-H<sub>2</sub>O, CaO-Al<sub>2</sub>O<sub>3</sub>-SiO<sub>2</sub>-H<sub>2</sub>O, CaO-Al<sub>2</sub>O<sub>3</sub>-SO<sub>3</sub>-CO<sub>2</sub>-Cl-H<sub>2</sub>O in the water and cement-based materials. In addition, Galíndez[7] used the reactive transport model to simulate the degradation of cementitious materials. These thermodynamic data allow the reactive transport model to simulate composition and concentration of chemical species under different hydrogeochemical environment. Table III lists the thermodynamic data that associate with described reactions of concrete degradation in a water-solid system of this study.

To assess the durability of cementitious materials of concrete barrier, a geochemical transport model

HYDROGEOCHEM 5.0 [8] was used to simulate reactive chemical transport processes involved in the concrete degradation in the near field. The computer program HYDROGEOCHEM 5.0 is a 3-D numerical model of fluid flow, thermal, hydrologic transport, and biogeochemical kinetic/equilibrium reactions in saturated/unsaturated media. HYDROGEOCHEM 5.0 is designed for generic applications to reactive transport problems controlled by both kinetic and equilibrium reactions in subsurface media. The effect of precipitation/dissolution on the change of pore size, hydraulic conductivity, and diffusion/dispersion are also incorporated. Detailed model description can be found in HYDROGEOCHEM 5.0 manual [8].

Table III Hydrogeochemical Reactions Considered in the HYDROGEOCHEM 5.0 Reactive Transport Model.

No.	Aqueous complexation reactions	Log K (25°C)
1	$\text{H}_2\text{O} = \text{OH}^- + \text{H}^+$	-14
2	$\text{Al}^{3+} + 4\text{OH}^- = \text{AlO}_2^- + 2\text{H}_2\text{O}$	33.12
3	$\text{Al}(\text{OH})_2^+ = \text{Al}^{3+} + 2(\text{OH})^-$	-3.41
4	$\text{Al}(\text{OH})_2^{2+} = \text{Al}^{3+} + (\text{OH})^-$	-9.05
5	$\text{Al}(\text{SO}_4)_2^- = \text{Al}^{3+} + 2\text{SO}_4^{2-}$	-4.9
6	$\text{AlSO}_2^+ = \text{Al}^{3+} + \text{SO}_4^{2-}$	-3.01
7	$\text{Ca}^{2+} + \text{HCO}_3^- + \text{OH}^- = \text{CaCO}_3 + \text{H}_2\text{O}$	6.895
8	$\text{Ca}^{2+} + \text{Cl}^- = \text{CaCl}^+$	-0.7
9	$\text{CaCl}_2 = \text{Ca}^{2+} + 2\text{Cl}^-$	0.64
10	$\text{CaHCO}_3^+ = \text{Ca}^{2+} + \text{HCO}_3^-$	-1.05
11	$\text{Ca}^{2+} + \text{OH}^- = \text{CaOH}^+$	-1.15
12	$\text{Ca}^{2+} + \text{SO}_4^{2-} = \text{CaSO}_4$	2.11
13	$\text{HCO}_3^- = \text{CO}_2(\text{aq}) + \text{OH}^-$	7.66
14	$\text{HCO}_3^- + \text{OH}^- = \text{CO}_3^{2-} + \text{H}_2\text{O}$	-3.67
15	$\text{HAlO}_2(\text{aq}) + \text{H}_2\text{O} = \text{Al}^{3+} + 3(\text{OH})^-$	-25.57
16	$\text{HCl} + \text{OH}^- = \text{Cl}^- + \text{H}_2\text{O}$	13.33
17	$\text{H}_4\text{SiO}_4 + 2\text{OH}^- = \text{H}_2\text{SiO}_4^{2-} + 2\text{H}_2\text{O}$	5
18	$\text{H}_2\text{SO}_4 + 2(\text{OH})^- = \text{SO}_4^{2-} + 2\text{H}_2\text{O}$	29.02

19	$\text{HSO}_4^- + \text{OH}^- = \text{H}_2\text{O} + \text{SO}_4^{2-}$	12.02
20	$\text{K}^+ + \text{Cl}^- = \text{KCl}$	-1.49
21	$\text{K}^+ + \text{OH}^- = \text{KOH}$	-0.46
22	$\text{K}^+ + \text{SO}_4^{2-} = \text{KSO}_4^-$	0.85
23	$\text{NaAlO}_2 + 2\text{H}_2\text{O} = \text{Al}^{3+} + \text{Na}^+ + 4\text{OH}^-$	-18.37
24	$\text{Na}^+ + \text{Cl}^- = \text{NaCl}$	-0.78
25	$\text{NaHCO}_3 = \text{HCO}_3^- + \text{Na}^+$	-0.15
26	$\text{Na}^+ + \text{H}_4\text{SiO}_4 + \text{OH}^- = \text{NaH}_3\text{SiO}_4(\text{aq}) + \text{H}_2\text{O}$	5.99
27	$\text{Na}^+ + \text{HCO}_3^- + \text{OH}^- = \text{NaCO}_3^- + \text{H}_2\text{O}$	4.19
28	$\text{Na}^+ + \text{OH}^- = \text{NaOH}$	-0.79
29	$\text{Na}^+ + \text{SO}_4^{2-} = \text{NaSO}_4^-$	0.82
30	$\text{HCO}_3^- + 9\text{H}^+ + 8\text{e}^- = \text{CH}_4(\text{aq}) + 3\text{H}_2\text{O}$	30.742
31	$2\text{H}_2\text{O} = \text{O}_2(\text{aq}) + 4\text{H}^+ + 4\text{e}^-$	-86.08
32	$2\text{H}^+ + 2\text{e}^- = \text{H}_2(\text{aq})$	-3.15
33	$\text{SO}_4^{2-} + 8\text{H}^+ + 8\text{e}^- = \text{S}^{2-} + 4\text{H}_2\text{O}$	20.732
34	$\text{SO}_4^{2-} + 9\text{H}^+ + 8\text{e}^- = \text{HS}^- + 4\text{H}_2\text{O}$	33.65
35	$\text{SO}_4^{2-} + 10\text{H}^+ + 8\text{e}^- = \text{H}_2\text{S} + 4\text{H}_2\text{O}$	40.644
36	$\text{Fe}^{+3} + \text{e}^- = \text{Fe}^{+2}$	13.02
37	$\text{Fe}^{+3} + 4\text{H}_2\text{O} = \text{Fe}(\text{OH})_4^- + 4\text{H}^+$	-21.6

No.	Mineral	Precipitation-dissolution reactions	Log K (25°C)	Molar volume (dm <sup>3</sup> /mole)
1	Calcite	$\text{HCO}_3^- + \text{Ca}^{2+} + \text{OH}^- = \text{CaCO}_3 + \text{H}_2\text{O}$	12.151	0.03693
2	Portlandite	$\text{Ca}^{2+} + 2\text{OH}^- = \text{Ca}(\text{OH})_2$	5.20	0.03300
3	Ettringite	$2\text{Al}^{3+} + 6\text{Ca}^{2+} + 26\text{H}_2\text{O} + 3\text{SO}_4^{2-} + 12\text{OH}^- = \text{Ca}_6\text{Al}_2(\text{SO}_4)_3(\text{OH})_{12} \cdot 26\text{H}_2\text{O}$	111.03	0.71032
4	Quartz	$\text{H}_4\text{SiO}_4 = \text{SiO}_2 + 2\text{H}_2\text{O}$	3.98	0.02269
5	Gypsum	$\text{Ca}^{2+} + \text{SO}_4^{2-} + 2\text{H}_2\text{O} = \text{CaSO}_4 \cdot 2\text{H}_2\text{O}$	4.58	0.07470
6	Hydrogarnet	$2\text{Al}^{3+} + 3\text{Ca}^{2+} + 12\text{OH}^- = \text{Ca}_3\text{Al}_2(\text{OH})_{12}$	87.68	0.14952
7	Friedel's salt	$2\text{Al}^{3+} + 4\text{Ca}^{2+} + 2\text{Cl}^- + 4\text{H}_2\text{O} + 12\text{OH}^- = 2\text{Ca}_2\text{Al}(\text{OH})_6\text{Cl} \cdot 2\text{H}_2\text{O}$	93.07	0.27624
8	Thaumasite	$3\text{Ca}^{2+} + \text{H}_4\text{SiO}_4 + \text{SO}_4^{2-} + \text{HCO}_3^- + 11\text{H}_2\text{O} + 3\text{OH}^- = \text{CaSiO}_3 \cdot \text{CaSO}_4 \cdot \text{CaCO}_3 \cdot 15\text{H}_2\text{O}$	31.70	0.32940
9	Monocarboaluminate	$2\text{Al}^{3+} + \text{HCO}_3^- + 4\text{Ca}^{2+} + 3.68\text{H}_2\text{O} + 13\text{OH}^- = 3\text{CaO} \cdot \text{Al}_2\text{O}_3 \cdot \text{CaCO}_3 \cdot 10.68\text{H}_2\text{O}$	101.45	0.26196
10	Pyrite	$\text{FeS}_2 + 2\text{H}^+ + 2\text{e}^- = \text{Fe}^{+2} + 2\text{HS}^-$	-18.479	0.02394

## SIMULATION OF CONCRETE DEGRADATION

The simulation region that has 40 m elevation at the bottom is discretized with 3918 elements and 4146 nodes. The grid comprises cells of dimensions  $\Delta x$ ,  $\Delta y$  varied from 1m to 0.1m, and  $\Delta z=2$ m. The vertical front edge, back edge and horizontal top edge depict no-flow boundary except the side ditch in vertical front edge. The side ditch area on front edge is set to a variable boundary condition, which is normally an air-media interface where water can seep out freely. The flux in bottom edge due to gravity is considered as a Neumann boundary with a zero flux. The horizontal left and right edges are Dirichlet head-boundary conditions. This hydraulic head value of Dirichlet boundary is estimated from the steady-state simulated groundwater flow (i.e.,  $V_x=4.0 \times 10^{-8}$  m/s, to left;  $V_z=3.3 \times 10^{-8}$  m/s, downward) in the proposed site of Arnold[9]. The estimated total head on the horizontal left and right edge nodes are assumed to be 420 dm and 432.8 dm, respectively.

As the repository start to operate, the cementitious materials of concrete of the EBS will interact with groundwater. To mitigate this type interaction, it is important to avoid the concrete immersion by the inflow of groundwater. A side ditch design is proposed by Taiwan Power Company to install at the bottom of the disposal tunnel and allow the drainage of inflow water. If the groundwater inflow is drained from the side ditch, the effect of concrete degradation on performance of EBS may be reduced. Hence, simulation scenarios considered herein are the performance assessment of EBS with and without side ditch. Table IV gives a summary of physical parameters for groundwater flow and reactive transport simulations. The study considers the hydrogeochemical transport of 11 components:  $\text{Na}^+$ ,  $\text{K}^+$ ,  $\text{Ca}^{2+}$ ,  $\text{Al}^{3+}$ ,  $\text{OH}^-$ ,  $\text{HCO}_3^-$ ,  $\text{Cl}^-$ ,  $\text{SO}_4^{2-}$ ,  $\text{H}_4\text{SiO}_4$ ,  $\text{Fe}^{3+}$ ,  $\text{e}^-$ , 37 aqueous species and 10 minerals of precipitation/dissolution reactions. Model simulation time is 300 years with initial time-step of  $1.0 \times 10^{-5}$  year, and maximum allowable time-step of 0.01 year. In addition, precipitation/dissolution on the change of porosity, hydraulic conductivity, and hydrodynamic dispersion of cementitious media may be a key hydrogeochemical mechanism in the concrete degradation. Thus, the effect of precipitation/dissolution reactions on both flow and reactive transport are also considered in the simulations. Moreover, to evaluate the effect of redox processes influencing on the formations of degradation materials, pyrite oxidation, sulfate reduction reactions are also incorporated in the simulation scenarios. Table V summarizes of initial and boundary conditions, and other parameters used in this study for reactive chemical transport modeling.

Table IV Physical Parameters Used in the HYDROGEOCHEM 5.0 Reactive Transport Model.

Media	K (m/s)	Porosity (%)	Diffusion coefficient (m <sup>2</sup> /s)	Bulk density (kg/m <sup>3</sup> )	Longitudinal dispersivity (m)	Lateral dispersivity (m)
concrete	$3.1 \times 10^{-14}$	0.15	$3.0 \times 10^{-12}$	2030	0.10	0.010
bentonite	$5.0 \times 10^{-11}$	0.363	$1.2 \times 10^{-10}$	2000	0.15	0.015
backfill	$3.24 \times 10^{-8}$	0.168	$2.0 \times 10^{-11}$	2410	0.30	0.030

Table V Initial and Boundary Conditions of Component Concentration (mole/l) Used in the Reactive Transport Model.

Component	I.C			B.C.
	Concrete	Bentonite	Backfill	Groundwater
Na <sup>+</sup>	6.908×10 <sup>-2</sup>	1.69×10 <sup>-1</sup>	1.01×10 <sup>-4</sup>	7.68×10 <sup>-5</sup>
K <sup>+</sup>	0.2665	1.14×10 <sup>-3</sup>	1.84×10 <sup>-6</sup>	1.84×10 <sup>-6</sup>
Ca <sup>2+</sup>	29.906	9.97×10 <sup>-3</sup>	3.61×10 <sup>-2</sup>	3.21×10 <sup>-2</sup>
Al <sup>3+</sup>	2.628	1.00×10 <sup>-20</sup>	3.33×10 <sup>-14</sup>	2.71×10 <sup>-8</sup>
OH <sup>-</sup>	21.1	1.91×10 <sup>-7</sup>	3.43×10 <sup>-7</sup>	3.43×10 <sup>-7</sup>
HCO <sub>3</sub> <sup>-</sup>	1.394×10 <sup>-11</sup>	2.14×10 <sup>-3</sup>	3.60×10 <sup>-4</sup>	3.81×10 <sup>-4</sup>
Cl <sup>-</sup>	5.64×10 <sup>-5</sup>	1.53×10 <sup>-1</sup>	1.79×10 <sup>-4</sup>	1.58×10 <sup>-4</sup>
SO <sub>4</sub> <sup>2-</sup>	1.633×10 <sup>-3</sup>	2.94×10 <sup>-2</sup>	8.57×10 <sup>-2</sup>	8.81×10 <sup>-2</sup>
H <sub>4</sub> SiO <sub>4</sub>	9.198	6.60×10 <sup>-5</sup>	1.51×10 <sup>-4</sup>	1.51×10 <sup>-4</sup>
Fe <sup>+3</sup>	3.10×10 <sup>-2</sup>	1.0×10 <sup>-8</sup>	1.0×10 <sup>-10</sup>	8.79×10 <sup>-4</sup>
pe	-1.0	-0.70	-1.0	-1.0

Three cases of reactive transport simulations are considered as follows:

Case 1: LLW repository without side ditch and redox processes

Case 2: LLW repository with side ditch and without redox processes

Case3: LLW repository with side ditch and redox processes

## RESULT AND DISCUSSION

The simulations of case 1, 2 and 3 were carried out using HYDROGEOCHEM 5.0. Simulated results showed significant differences in concrete degradation. Figure 2 illustrates the steady state distribution of flow velocity of case 1, 2 and 3. High groundwater inflow rate was developed quickly and drained out to the side ditch in case 2. The highest groundwater velocity of case 2 and 3 is 5.7 times greater than that of case 1.

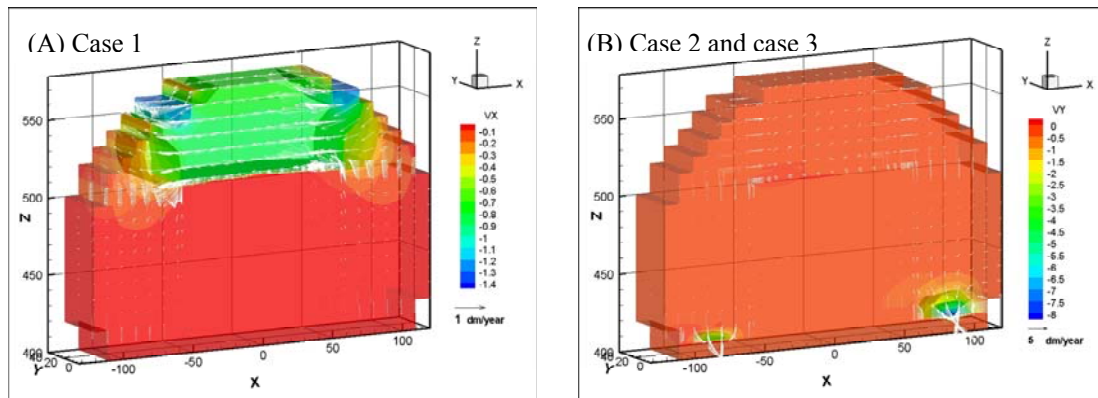


Fig. 2 Velocity distribution of steady state flow for case 1, case 2 and case 3.

In case 1, the ettringite was formed with maximum amount of about  $2.49 \times 10^{-2}$  mol/l at the edge of the vertical left, right and horizontal top edge areas of concrete barrier in 100 years. After 300 years, as shown in Figure 3(A), the amount of precipitated ettringite increases with time, reaching a maximum value of  $7.01 \times 10^{-2}$  M due to continuous sulfate intrusion. Nevertheless, the ettringite was mildly formed in case 2 with a amount of  $1.53 \times 10^{-4}$  M precipitated at top right edge of concrete barrier after 300 years as (Figure 3(B)).

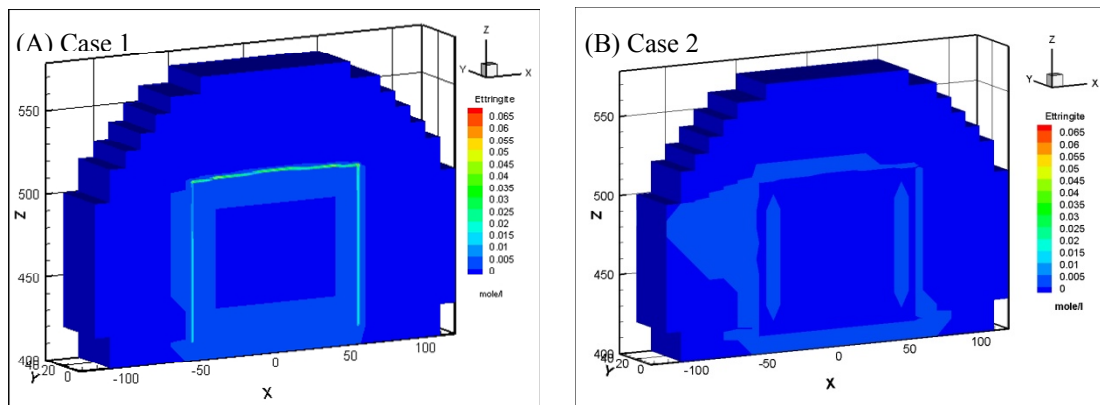


Fig. 3 Ettringite distribution for case 1 and case 2 after 300 years.

In case 1, the maximum amount was about  $2.94 \times 10^{-1}$  mol/l of Friedel's salt formed at the vertical left, right edge and horizontal top edge areas of concrete barrier in 100 years. The amount of Friedel's salt increases with time, and reach to a maximum value of about  $2.70 \times 10^{-1}$  M in 300 years. Nevertheless, in case 2 the Friedel's salt was formed with a amount of  $2.23 \times 10^{-1}$  M at vertical left edge of concrete barrier after 300 years. In addition, the Friedel's salt depleted in the area of top right edge. The amounts of portlandite precipitated in the case 1 and 2 were similar. The portlandite formed all over the concrete barrier in less than 300 years. Portlandite remains stable at all time. In case 2, the pH undergoes small change due to the interaction between groundwater and the cementitious minerals in concrete barrier. Initially the pH is close to 12, as the simulation proceeds hydrogen ion plume intruded, the pH decrease to 11.5 after

300 years. Small amount calcium in the cementitious minerals of concrete barrier was depleted. The amount and distribution of hydrogen ion, sulfate, and chloride species in the EBS showed significant differences in case 1 and case 2. The amount of these species in case 1 was one order of magnitude higher than that of in case 2. Thaumasite and monocarboaluminate also formed as carbonate aggregates by sulfate attack, and carbonate intrusion, respectively. Main processes responsible for concrete degradation are species induced from hydrogen ion, sulfate, and chloride. The concentrations of the hydrogen ion, sulfate, and chloride species in the EBS are affected by the rate of advective transport of groundwater outflow to the side ditch drainage system. Concentrations of hydrogen ion, sulfate, and chloride in the EBS with side ditch are lower than that of the EBS without side ditch. The side ditch efficient drains groundwater and lowers the concentration of the species induced concrete degradation of 300 years. EBS with the side ditch could divert the water and reduced the concrete degradation. The ettringite was also formed in case 3 with a small amount of  $2.86 \times 10^{-4}$  M precipitated at top right edge of concrete barrier after 300 years (Figure 4(A)). As the simulation continuously proceeds, the ettringite formation in case 3 after 600 years was still much less than that of in case 2 after 300 years (Figure 4(B)). In case 3, the redox processes controlled the geochemical reactions, such as pyrite oxidation, sulfate reduction concomitantly occurred in the concrete degradation processes. Appelo[10] pointed out that ongoing sulfate reduction can be recognized by the presence of  $H_2S$  in groundwater. Figure 4(C) and 4(D) show that  $H_2S$  was formed at left, top and right edge of concrete barrier. Thus, sulfate reduction reduced the concentration of sulfate and ettringite formation. Therefore, the redox processes in the EBS can reduce the ettringite formation in the concrete degradation processes.

This study considers limited chemical reactions under chemical equilibrium condition, more comprehensive reactions of cementitious phase and the chemical kinetics should be included in the future reactive chemical transport simulations. Judging from the simulated results, the hydrogen ion can result in dissolution of portlandite and increases the concentration of calcium in the pore water. The sulfate anion reacts with cement to form ettringite. The chloride from the pore water enters the cementitious materials to form the Friedel's salt. Luna et al.[3] pointed out that the ettringite can cause the volumetric expansion and eventually lead to fracturation processes. Excess of chlorite can produce corrosion of the reinforcement element and causes a volume expansion which may lead to micro-fracturing in the concrete. Formation of ettringite, and Friedel's salt are also associated to a volume increase eventually leading to fracture formation and weaken the EBS. Seitz and Walton[11] show the detail failure mechanisms for concrete vaults. They pointed out that as cracks fully penetrate the concrete, the permeability of the vault increases. Cracks can also accelerate degradation rates. Thus, water flow through cracks over extended periods is the primary concern for concrete performance of long life radionuclides[11]. Moreover, seismic fractures may induce the coincided cracks and increase permeability. HYDROGEOCHEM 5.0 is not able to simulate cracks damage, or its impact on permeability. Further quantification of concrete degradation by coincided concrete cracks and numerical model coupled with thermo-hydraulic-mechanical-chemical processes is suggested to be developed in the future.

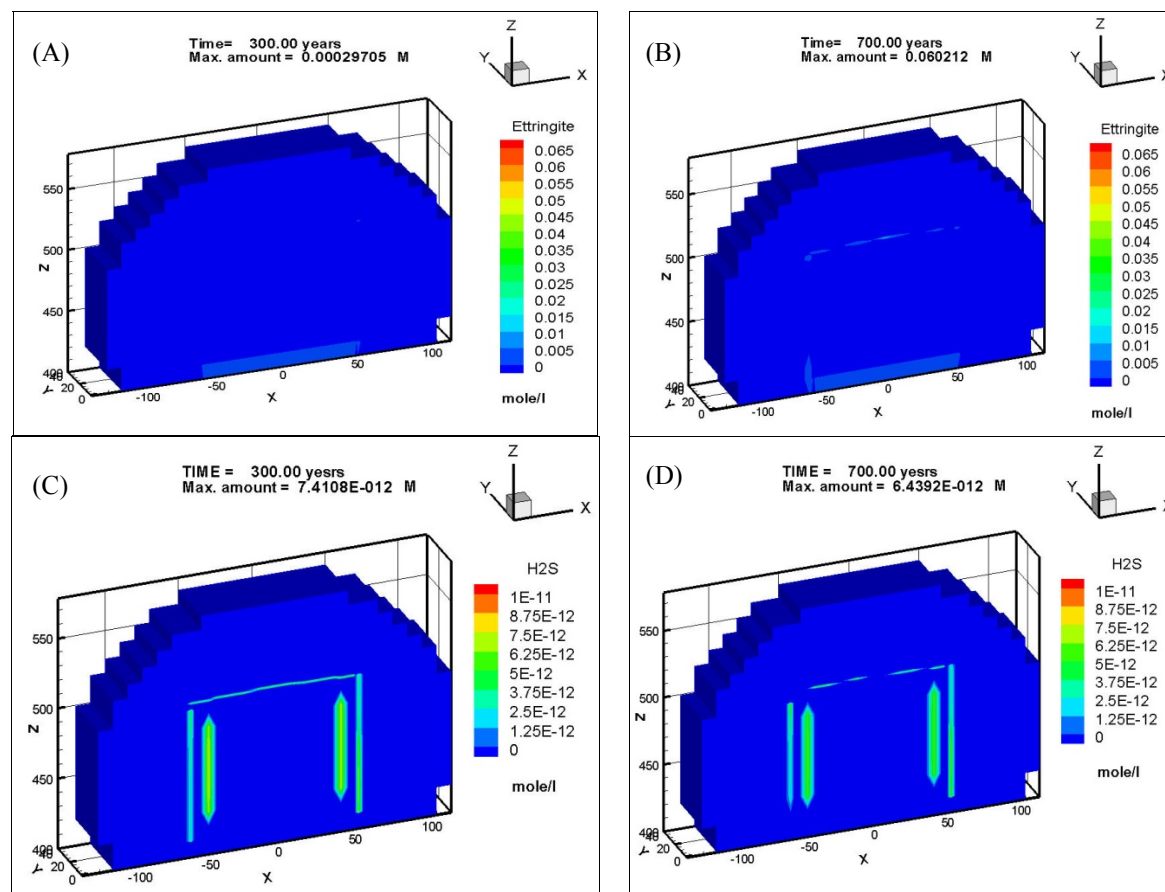


Fig. 4 Distribution of ettringite and hydrogen sulfide for case 3 after 300 and 700 years: (A) Ettringite 300 years, (B) Ettringite 700 years, (C) Hydrogen sulfide 300 years, and (D) Hydrogen sulfide 700 years.

## CONCLUSION AND SUGGESTION

A proposed site for final disposal of LLW of Daren is on the selected list in Taiwan. To investigate the hydrogeochemical reactions and effect on concrete degradation in the proposed LLW repository site, HYDROGEOCHEM5.0 model was applied to simulate the complex chemical interactions between the cement minerals of the concrete and groundwater flow and reactive chemical transport resulting from water-rock interaction in the proposed site. Simulation results show the main processes responsible for concrete degradation are geochemical reactive species induced from hydrogen ion, sulfate, and chloride. The intrusion of hydrogen ion from groundwater results the dissolution of portlandite. However, the portlandite still maintains alkaline condition in proposed LLW repository, the concrete used as a confinement material in EBS may remain in well durable condition. The sulfate-induced concrete degradation may form the ettringite and the chloride-induced concrete degradation form Friedel's salt. Thaumasite and monocarboaluminate are also formed as carbonate aggregates by sulfate attack, and carbonate intrusion, respectively. The formation of ettringite, Friedel's salt, thaumasite and monocarboaluminate may result a volume expansion. The EBS with the side ditch efficiently drains the ground water and lowers the

concentration of concrete degradation induced species. The degree of concrete degradation on performance of EBS with side ditch is much lower than the disposal tunnel without the side ditch. Moreover, the redox processes significantly influence on the formations of degradation materials. Reductive environment in the EBS can reduce the ettringite formation in the concrete degradation processes.

The results of the study provide a detail picture of the long-term evolution of the hydrogeochemical environment of the proposed LLW disposal site in Taiwan. The chemical kinetics effect should be included in future reactive chemical transport simulations. Moreover, the interaction among water and other minerals of cement, bentonite, and backfill materials in the near field, volume-expanded cracks and seismic induced-fractures should be also considered in the future research. The development of advanced numerical models that coupled with thermo-hydraulic-mechanical-chemical processes is especially welcomed.

## **ACKNOWLEDGEMENT**

The authors are grateful to the National Science Council, Republic of China, for financial support of this research under contract No. NSC 98-3114-E-002-013, NSC 98-3114-E-007-015 and NSC 99-NU-E-002-003.

## **REFERENCES**

1. TAIWAN POWER COMPANY, *Performance assessment in low-level radioactive waste disposal facility, version B, (in Chinese)*, p. 513, Taiwan Power Company (2010).
2. B. LAGERBLAD, J. TRÄGARDH, *Conceptual model for concrete long time degradation in a deep nuclear waste repository*, p. 104, Swedish Cement and Concrete Research Institute, SKB TR 95-21, (1994).
3. M. LUNA, D. ARCOS, L. DURO, *Effects of grouting, shotcreting and concrete leachates on backfill geochemistry*, p. 51, Svensk Kärnbränslehantering AB, SKB R-06-107 (2006).
4. J. BRUNO, D. ARCOS, L. DURO, *Processes and features affecting the near field hydrochemistry: Groundwater-bentonite interaction*, p. 56, Svensk Kärnbränslehantering AB, SKB TR-99-29 (1999).
5. PH. BLANC, X. BOURBON, "A. Lassin, E. C. Gaucher, Chemical model for cement-based materials: Thermodynamic data assessment for phases other than C-S-H," *Cement and Concrete Research*, **40**, 1360 (2010a)
6. PH. BLANC, X. BOURBON, "A. Lassin, E. C. Gaucher, Chemical model for cement-based materials: Temperature dependence of thermodynamic functions for nanocrystalline and crystalline C-S-H phases," *Cement and Concrete Research*, **40**, 851 (2010b)
7. J. M. GALÍNDEZ, J. MOLINERO, "On the relevance of electrochemical diffusion for the modeling of degradation of cementitious materials," *Cement & Concrete Composites*, **32**, 351 (2010).
8. G. T. YEH, J. SUN, P. M. JARDINE, W. D. BURGOS, Y. FANG, M. H. LI AND M. D. SIEGEL, *HYDROGEOCHEM 5.0: A three-Dimensional model of coupled fluid flow, thermal transport, and hydrogeochemical transport through variably saturated conditions – version 5.0*, p. 243, ORNL/TM-2004/107,

**WM2011 Conference, February 27 - March 3, 2011, Phoenix, AZ**

Oak Ridge National Laboratory, Oak Ridge, TN (2004).

9. B. W. ARNOLD, R. G. KNOWLTON, F. J. SCHELLING, P. D. MATTIE, J. C. COCHRAN, H. N. JOW, *Taiwan Industrial Cooperation Program Technology Transfer for Low-Level Radioactive Waste Final Disposal – Phase I*, p. 148, Sandia National Laboratories, SAND2007-0131, (2007).
10. C. A. J. APPELO, D. POSTMA, *Geochemistry, groundwater and pollution*, 2nd edition, p. 649, A. A. BALKEMA PUBLISHERS A.A. Balkema Publishers, Leiden, The Netherlands (2005).
11. R. R. SEITZ, J. C. WALTON, *Modeling approaches for concrete barriers used in low-level waste disposal*, p. 22, NUREG/CR-6070 (1993).